SAND98-2635C

# PROBABILISTIC ANALYSIS OF RECHARGEABLE BATTERIES IN A PHOTOVOLTAIC POWER SUPPLY SYSTEM

Angel Urbina
Sandia National Laboratories
Experimental Structural Dynamics, 9119
Mail Stop 0557
Albuquerque, NM 87185-0557

Rudolph Jungst, David Ingersoll
Sandia National Laboratories
Lithium Battery R&D Department, 1521
Mail Stop 0613
Albuquerque, NM 87185-0613

Thomas L. Paez, Christian O'Gorman, Patrick Barney
Sandia National Laboratories
Experimental Structural Dynamics, 9119
Mail Stop 0557
Albuquerque, NM 87185-0557



## ABSTRACT

We developed a model for the probabilistic behavior of a rechargeable battery acting as the energy storage component in a photovoltaic power supply system. Stochastic and deterministic models are created to simulate the behavior of the system components. The components are the solar resource, the photovoltaic power supply system, the rechargeable battery, and a load. Artificial neural networks are incorporated into the model of the rechargeable battery to simulate damage that occurs during deep discharge cycles. The equations governing system behavior are combined into one set and solved simultaneously in the Monte Carlo framework to evaluate the probabilistic character of measures of battery behavior.

## INTRODUCTION

A rechargeable battery energy storage system is essential for making the power from a photovoltaic system dispatchable. A photovoltaic-based power supply system sizes power generation to satisfactorily service the system load (if, indeed, load exists while the photovoltaic system generates power) and charge an energy storage system (typically, a lead-acid battery) that will service the system load when the photovoltaic system is not generating power. The system is optimally sized when, over the long term: (1) The photovoltaic component generates sufficient power to service the load and simultaneously generate sufficient stored energy to service the load when it is not operating, and (2) the rechargeable battery has sufficient capacity to avoid lengthy periods of time at a low state of charge. Discharge cycles that drain lead acid batteries below a threshold level for a time duration beyond a threshold value accumulate damage in the batteries. This damage is manifest by a diminution of maximum possible battery capacity. Cost constraints and the variability of the photovoltaic output, depending on weather conditions, make it impractical to overdesign the system sufficiently to entirely avoid periods of deficit charging. A predictive capability for the performance of the battery under the various design options is needed to optimize the system for the best tradeoff among cost, load requirements, and battery life.

## DISCLAIMER

The present investigation creates a model for maximum battery capacity and cycle life using an artificial neural network (ANN). Specifically data obtained either experimentally or synthetically are used to create an ensemble of data that serves as exemplars for training the ANN. These ensembles contain various discharge profiles, including periods of deep discharge, for a particular type of battery. The ANN is used to reckon damage to potential maximum battery capacity caused by deep discharge. In summary, battery damage is modeled as deterministic.

The power supplied by the photovoltaic system is modeled as a stochastic process. Because solar insolation varies randomly as a function of time and is equal to or less than some theoretical maximum value, the stochastic process, typically, does not have a probability density function that is symmetric in its states and, therefore, is not modeled as Gaussian. In this work an approach that employs a Markov process is used to simulate components of the solar data. The load is modeled as deterministic in this study.

All these elements are combined into a single framework to yield a stochastic model for the photovoltaic power supply and energy storage system. The model is operated on the Monte Carlo principle to yield realizations of the stochastic processes characteristic of the operational phenomena, and these can be analyzed using the tools of classical statistics and random signal analysis to infer the probabilistic behavior of the system. Ultimately the model can be used to design and optimize the power supply system.

Mathematical descriptions of subsystem behavior are presented in the following section along with some relations required to describe system interactions. Next a numerical example is presented. Finally, some conclusions are drawn and presented.

## MATHEMATICAL MODEL OF A POWER SUPPLY/STORAGE/LOAD SYSTEM

Our objective is to model and simulate a renewable energy supply and storage system. The particular system consists of four parts: a solar resource model, a photovoltaic power conversion model, a rechargeable battery energy storage model, and a load model. We provide the details of the individual subsystem models then combine the components into a model of the overall system. The solar resource is modeled as a random process, and we develop the capability to generate realizations of the solar radiation from the random source. These realizations are used as the system input, along with a deterministic load, that drives response in the battery storage system. Equations that permit simulation of battery behavior are solved for specific load and insolation inputs, and the results are used in a Monte Carlo framework to characterize system behavior.

### The Solar Resource Model

The first subcomponent to be modeled is the power source of the photovoltaic system: the sun. The amount of solar energy available on a given surface area is particularly important. This is the solar insolation, and it is measured in units of power per area-i.e., units of W-hr/$m^2$, BTU/$ft^2$-hr, etc. There exist many sets of measured data that are readily available from local, state, and federal agencies. These data include values of global, direct, and diffuse solar radiation (either measured with a pyranometer or calculated) and can be used to calculate the solar energy received by a solar array (or collector) (1) or to guide the development of an insolation model. A model was developed to calculate the solar energy received by a flat plate collector tilted at an angle and located at arbitrary latitude. Equation 1 identifies fundamental quantities and their relation:

$$E_o = E_{bc} + E_d + E_{gr} \quad [1]$$

where $E_o$ is the total solar energy received by an inclined plane, $E_{bc}$ is the direct beam contribution, $E_{gr}$ is the ground reflected energy, and $E_d$ is the diffuse (or sky) energy (2). Each term, along with its relation to more fundamental quantities, is developed in the following.

The direct beam contribution ($E_{bc}$) is defined by Equation 2:

$$E_{bc} = E_{dn} \cos(\theta) \quad [2]$$

where $E_{dn}$ is the direct normal solar radiation (hourly values available in data bases) as measured with a pyranometer; it is defined as that radiation received within a 5.7° field of view centered on the sun, and $\theta$ is the incident angle of the sun's rays to the collector (2). The incident angle is a function of the latitude at which the collector is located, its tilt angle, and the position of the sun in the sky. A detailed explanation of how this value is obtained can be found in Kreider and Kreith (3).

The diffuse radiation model is described by Equation 3:

$$E_d = E_{dh}\left\{0.5(1-F_1)(1+\cos\beta)+F_1\left(\frac{a}{b}\right)+F_2\sin\beta\right\} \quad [3]$$

where $E_d$ is the diffuse (sky) radiation and $E_{dh}$ is the diffuse horizontal solar radiation (hourly values available in data bases) as measured with a pyranometer. $E_{dh}$ is defined as that radiation received from the sky (excluding the solar disk) on a horizontal surface, $F_1$ and $F_2$ are coefficients associated with the condition of the sky, a and b are functions of the position of the sun in the sky, and $\beta$ is the tilt angle of the collector (as measured from the horizontal). Equation (3) is also referred to as the Perez Model. A detailed explanation of its development and further discussion of the various parameters can be found in Perez et al. (4).

The final component in Equation (1) is represented by Equation (4):

$$E_{gr} = 0.5\rho E_h(1+\cos\beta) \quad [4]$$

where $E_{gr}$ is the ground reflected radiation, $\rho$ is the surface reflectivity or albedo, and $E_h$ is the global horizontal solar radiation values. $E_h$ is defined as the total radiation-i.e., direct and diffuse received on a horizontal surface; and $\beta$ is the tilt of the collector (from the horizontal). Albedo values range from 0.2 for green vegetation and some soils, 0.35 for old snow, and up to 0.95 for dry new snow (2).

Because the ground reflected radiation can be characterized as a function of the direct normal radiation and the diffuse horizontal radiation, we model the latter two in the following.

## Synthetic Generation of Solar Data Using a Markov Process

Consideration of the measured insolation data indicates that the direct normal radiation and the diffuse horizontal radiation are random processes that are statistically dependent and non-Gaussian. We reach these conclusions through consideration of, for example, the data in Figure 1. This is a plot of 310 joint realizations of diffuse horizontal radiation versus direct normal radiation at 11:00 AM on 310 separate January days.

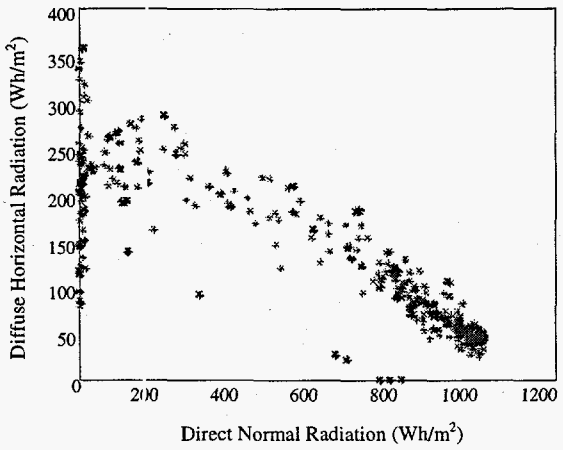


Figure 1: Joint realizations of diffuse and direct radiation

The fact that the joint realizations are not distributed within a circular or elliptical area combined with our intuition about the physics of the problem lead to the former conclusion–that is, the random processes are statistically dependent. Figures 1a and 1b are the kernel density estimators (KDE) of the diffuse horizontal radiation and the direct normal radiation, respectively. The fact that these estimated probability density functions (PDF) are far from normal leads to the second conclusion: that the random processes are non-Gaussian. [For more information on KDEs, see Silverman, (5)].

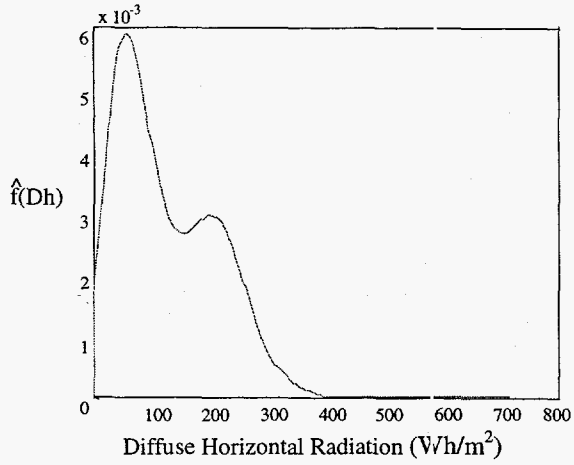


Figure 1a: KDE of the diffuse radiation

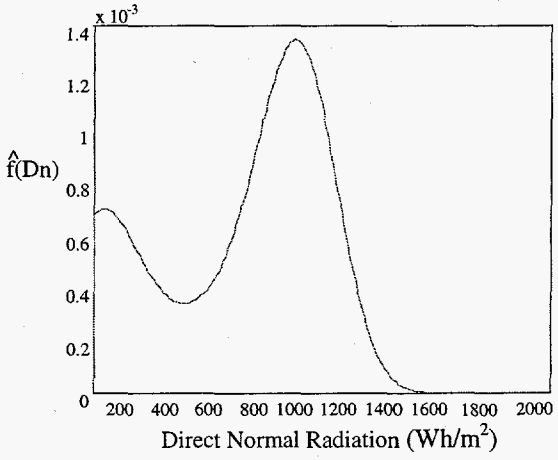


Figure 1b: KDE of the direct radiation

To accommodate these facts and to reflect our belief that the dependence of the random processes upon their histories can be accounted for using one-step-memory, we choose to model the joint behavior of the random processes with a bivariate, first order Markov chain. [See Isaacson and Madsen (6), for example, for an introductory discussion of Markov chains.] A Markov chain is a special type of Markov random process with discrete states and discrete parameter. The parameter is, in this case, time index. The bivariate state of the random process is the joint values of diffuse horizontal radiation and direct normal radiation. The underlying framework for the Markov chain creates bins for the joint values of the diffuse horizontal radiation and the direct normal radiation at each hour and identifies the system state according to the bin occupied by the radiation value at that hour. The probability mass function (PMF) specifying the chance that the system state occupies a particular bin at a particular hour is known as the state probability. The objective in use of the Markov chain is to determine the state probabilities at all times, for all measures of behavior of interest, for the system under consideration. This is accomplished, in the Markov chain framework, by specifying the initial

state PMF, estimating (or otherwise deriving) the transition PMF (to be described in the sequel), and using the two to propagate state probabilities through time.

Consider Figure 2 for a hint as to how the construct described in the previous paragraph can be developed. It shows the same data as Figure 1 but, in addition, separates the data into bins. The bin sizes are arbitrary and spatially disjoint. They cover the entire set of measured data. The location of radiation data within each bin can be approximated as the bin centroid location. Each bin can be indexed, for reference purposes for example, by starting at the lower left corner and moving up the columns. Figure 3 shows 310 joint realizations of diffuse horizontal radiation and direct normal radiation at 12 noon on the same 310 days represented in Figure 2. Each datum in Figure 3 corresponds to a particular datum in Figure 2-that is, each joint realization at 11:00 AM propagates into a joint realization at 12 noon. The data in Figure 3 are binned as the data in Figure 2 were, but the bin boundaries differ, as they must, to cover the different range of all the joint realizations. There are as many bins in Figure 3 as there are in Figure 2.

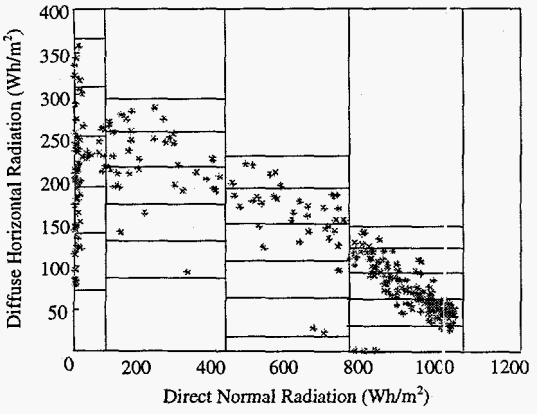


Figure 2: Bins for data at 11:00 AM

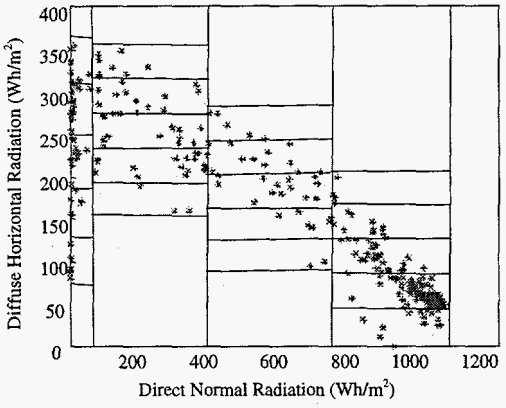


Figure 3: Bins for data at noon

It is clear that any of a number of statistical estimation approaches can be used to find the probability that the joint realization of the diffuse horizontal radiation and the direct normal radiation random process moves from a particular state to any other state during the course of an hour. Though a simple statistical estimation procedure was used in this study, its description is beyond the scope of this paper. In addition, an initial state PMF can be easily identified; the joint state always starts the day with joint radiation of zero.

The Markov chain is formally constructed as follows. Denote the vector random process under consideration as $\{\boldsymbol{X}_j, j = 0, \ldots n - 1\}$, where $j$ is the time index. In this particular case each vector random variable in the random process, $\boldsymbol{X}_j$, consists of two random scalar variables: the diffuse horizontal radiation and the direct normal radiation at time index $j$. The state probabilities of the Markov chain are denoted $\boldsymbol{p}_j$, $j = 0, \ldots n - 1$ and contain the following information.

$$\boldsymbol{p}_j = \begin{Bmatrix} P(\boldsymbol{X}_j = \boldsymbol{s}_1) \\ P(\boldsymbol{X}_j = \boldsymbol{s}_2) \\ \vdots \\ P(\boldsymbol{X}_j = \boldsymbol{s}_N) \end{Bmatrix} \qquad j = 0,\ldots,n-1 \qquad [5]$$

where $P(.)$ indicates the probability of the event described in parentheses, and the $\boldsymbol{s}_i$, $i = 1,\ldots, N$, are the states of the Markov chain-i.e., for example, the centroids of the bins in Figure 2 or Figure 3. The PMF of initial states is $\boldsymbol{p}_0$.

The probabilities that the bivariate Markov chain evolves from any state at time index $j$ to the same state or any other at time index $j$+1-i.e., during the course of an hour-are encapsulated in the transition probability matrix, denoted $\boldsymbol{P}_{j+1|j}$. This matrix contains the following information.

$$\boldsymbol{P}_{j+1|j} = \begin{bmatrix} P\left(X_{j+1}=s_1 \middle| X_j=s_1\right) & P\left(X_{j+1}=s_1 \middle| X_j=s_2\right) & \cdots & P\left(X_{j+1}=s_1 \middle| X_j=s_N\right) \\ P\left(X_{j+1}=s_2 \middle| X_j=s_1\right) & P\left(X_{j+1}=s_2 \middle| X_j=s_2\right) & \cdots & P\left(X_{j+1}=s_2 \middle| X_j=s_N\right) \\ \vdots & \vdots & \ddots & \vdots \\ P\left(X_{j+1}=s_N \middle| X_j=s\right) & P\left(X_{j+1}=s_N \middle| X_j=s_2\right) & \cdots & P\left(X_{j+1}=s_N \middle| X_j=s_N\right) \end{bmatrix}$$

$$j=0,\ldots,n-2 \qquad [6]$$

where $P\left(X_{j+1}=s_{i_2} \middle| X_j=s_{i_1}\right)$ is the conditional PMF denoting the chance that the system moves to state $i_2$ at time index $j$+1, given that it occupied state $i_1$ at time index $j$. As mentioned above, these conditional probabilities can be estimated from measured data, but the procedure for doing so will not be presented here. We will simply add that the data are used to establish hour-to-hour transition probabilities, and this is done on a monthly basis. So with ten years of data, 310 realizations of hour-to-hour transitions are available for days in January, and these can be used to estimate hour-to-hour transition probabilities for January days. The other months are treated similarly.

Some attractions of the Markov chain framework for analyses are: (1) that the state probabilities need not follow a normal law and (2) that the procedure for propagation of the state probabilities is simple, fast, and efficient. To establish the state probabilities at time index $j$+1, we use the formula

$$\boldsymbol{p}_{j+1} = \boldsymbol{P}_{j+1|j}\boldsymbol{p}_j \qquad j=0,\ldots,n-2 \qquad [7]$$

Clearly then knowledge of the initial state PMF and the transition probability matrices in Eq. (6) is sufficient to compute the state probabilities at time indices $j$=1,…,$n$-1.

We choose to use the Markov chain model in a Monte Carlo framework in the analyses to follow. This means that realizations of the bivariate random process that models the diffuse horizontal radiation and the direct normal radiation must be generated. To accomplish this, we select a starting state at random, following the PMF of initial states, from among the potential starting states. To do this, we generate a uniformly distributed random variate in [0,1] and select the starting state as the one whose cumulative probability corresponds to the random variate. We then set all the values in $\boldsymbol{p}_0$ to zero, except for the state that is the chosen starting state; that probability is set to one. We then pre-multiply $\boldsymbol{p}_0$ by $\boldsymbol{P}_{1|0}$ to obtain $\boldsymbol{p}_1$, the state PMF at time index 1. We select a realization from among the possible states by generating a uniformly distributed random variate in [0,1] and selecting the state as the one whose cumulative probability corresponds to the random variate. We continue this process throughout the n-step duration of the random process to obtain a realization of the diffuse horizontal radiation and the direct normal radiation. As many realizations of the random process as desired can be generated in this way.

## The Photovoltaic Power Supply Model

The power to this system is supplied by a photovoltaic array that transforms the solar insolation into dc current at a specified voltage. Because of the complex behavior of these polycrystalline silicon arrays, a number of models have been proposed to relate the insolation

input to the expected output of the arrays. Some of these models take into account the cell's physical characteristics-i.e. temperature, chemical composition, etc.-and the location's ambient conditions. For this project a specific type of photovoltaic array was selected, and its maximum rated current output was used to determine the current produced at a particular time. In other words, given the maximum rated current of the photovoltaic array, $I_{mp}$, (which we will consider a constant) and the solar insolation, $E_0$(t) at time t, the current produced by the array is given by

$$I(t) = I_{mp} \cdot E_0(t) / C_0 \qquad [8]$$

where $C_0$ is the energy per square meter applied to the collector over a computational time increment, at which the current $I_{mp}$ is generated. A time history of hourly current values can be obtained by using the output of Equation (1) in Equation (8).

## The Load Model

The load model appropriate to the analysis of a particular system depends on the particular use that the photovoltaic power supply system is intended to serve. It could vary from a very simple deterministic system to a complex stochastic power distribution grid. The load used in this investigation is defined as a lighting system operated only during the nighttime. ` The current demanded by the load at a specified voltage is denoted $I_L(t)$.

## The Rechargeable Battery Model

The focus of the overall investigation is to characterize the probabilistic behavior of rechargeable batteries that are recharged from a renewable source that provides power in random increments. Further, we narrow our focus more by concentrating on the damage that can accumulate in rechargeable batteries, specifically lead acid batteries, when they are subjected to deep discharge use cycles. In particular it is known that when rechargeable batteries are used at a low state of charge, the maximum potential capacity can be diminished. This may eventually lead to battery failure. In view of these things, we develop a framework to model battery state of charge and maximum potential battery capacity as functions of time. We introduce the damage effect that occurs during deep discharge via a non-positive function of duration of deep discharge and depth of deep discharge. Because the form of this function is unknown, we model it with an artificial neural network (ANN) whose parameters are to be trained with experimental data. (This training has not yet been accomplished, so for now the ANN model has been trained with data we consider plausible.) O'Gorman et al., (7) first demonstrated the use of ANNs to simulate battery performance.

We introduce notation for the current demanded from the battery, $I_B(t)$, and the recharge current available to the battery, $I_R(t)$, for use in the development of the system's governing equations. In terms of these quantities, the state of charge in the rechargeable battery system can be expressed

$$C(t) = \begin{cases} \int_{t_0}^{t} \gamma(\tau)[I_R(\tau) - I_B(\tau)]d\tau + C(t_0) & t \geq t_0, \quad C(t) \leq M_C(t) \\ M_C(t) & otherwise \end{cases} \qquad [9]$$

The function $M_C(t)$ is the maximum potential battery capacity at time $t$. The function $\gamma(t)$ is the recharge efficiency that establishes the rate at which recharge can occur. In general, as a rechargeable battery nears its maximum potential capacity, $\gamma(t)$ approaches zero, and at lower

levels $\gamma(t)$ is near one. Battery testing would be required to establish the specific form and parameters of this function. For present purposes we arbitrarily take the function to be

$$\gamma(t)=\begin{cases}1 & C(t)/M_C(t)<\alpha, \quad \alpha\in(0,1) \\ 0.5\left[1-\cos\pi\left(1+\dfrac{(C/M_C)-\alpha}{1-\alpha}\right)\right] & \alpha\le C(t)/M_C(t)\le 1\end{cases} \qquad [10]$$

This function has the graph shown in Figure 4 for $\alpha = 0.85$.

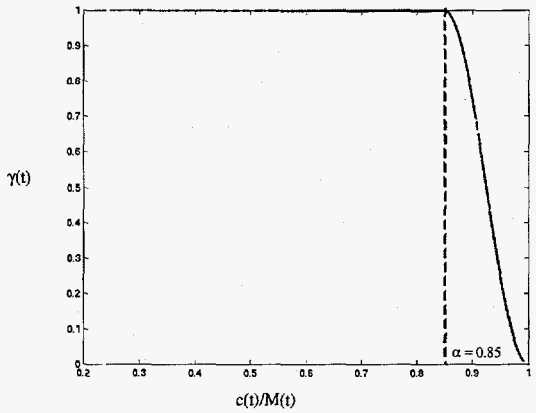


Figure 4: Recharge efficiency curve

Because the function $M_C(t)$ tracks the maximum potential battery capacity as a function of time and because we take damage to a rechargeable battery (when used in photovoltaic application) caused by deep discharge as irreversible, $M_C(t)$ must be a monotone non-increasing function. We choose the following as the form for $M_C(t)$:

$$M_C(t)=\int_{t_0}^{t}\delta_M(\tau)d\tau+M_C(t_0) \qquad t\ge t_0 \qquad [11]$$

The function $\delta_M(t)$ must be non-positive and must indirectly characterize damage to the maximum potential capacity of the rechargeable battery during deep discharge. For present purposes we assume that $\delta_M(t)$ is a function of the time duration of a discharge below a threshold, $T(t)$, and the depth of discharge below a threshold, $D(t)$. Therefore, we write

$$\delta_M(t)=g_\delta(T,D) \qquad [12]$$

We specify that $g_\delta(T,D)$ is zero for $T(t)$ below its threshold value or $D(t)$ below its threshold value, but beyond this we do not know the form of $g_\delta(T,D)$. It is anticipated that an explicit form for $g_\delta(T,D)$ cannot be easily derived, so we choose to model the function using an ANN. Any of a number of robust forms can be used here including, for example the layered perceptron ANN (see Freeman and Skapura, 1992 (8)) or the radial basis function ANN (see Moody and Darken, 1989 (9)). In the numerical example to follow, we use a particular form of the layered perceptron ANN to model $g_\delta(T,D)$. The advantage in using an ANN here is that given sufficient training data, it learns rapidly. Further, ANNs are accurate and efficient. The ANN used to model $g_\delta(T,D)$ in this investigation is shown in Figure 5. This model will be only applicable to the particular type of battery used in this project.

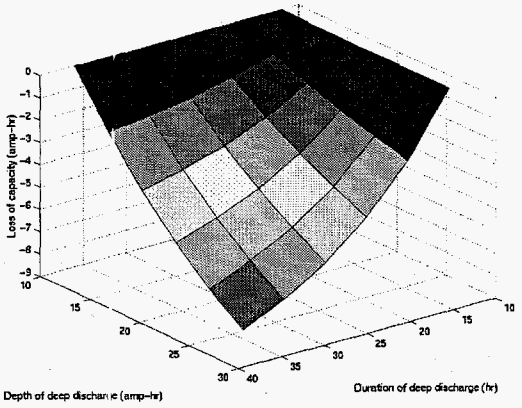


Figure 5: ANN model of battery damage

There are two practical issues that must be resolved before the equations governing battery behavior can be implemented. First, as deep discharge of the rechargeable battery occurs, a smoothing must be applied to the state of charge in order for sensible realizations of the function $g_\delta(T,D)$ to be modeled. We choose to apply a one-day moving average of the state of charge in our definition of $D(t)$. Second, we seek to keep track of the maximum potential capacity of the battery at all times; however, when the system is in the midst of a deep discharge cycle, the ultimate duration of the cycle is unknown. To accommodate this fact, once a deep discharge cycle has commenced, we estimate its ultimate duration by noting the present state of the system and assuming that the state of charge will recover at the average rate of recharge.

## Combined Mathematical Model

Upon the addition of two equations relating photovoltaic production and load demand to battery recharge and discharge, the equations governing subsystem behavior can be combined into a single, simultaneous set of equations to simulate the behavior of the overall system. Previously $I_L(t)$ was defined as the current demand at the load, $I_{PV}(t)$ was defined as the current available from the photovoltaic system, and $I_B(t)$ was defined as the current demand on the battery. These quantities are related via Equation (13)

$$I_B(t) = H[I_L(t) - I_{PV}(t)](I_L(t) - I_{PV}(t)) \qquad [13]$$

where $H[.]$ is the Heaviside unit step function. This indicates that the current demand on the battery is a linear function of the excess of the load demand beyond capability of the photovoltaic system to supply it. The current demand on the battery is zero when the load does not exceed the photovoltaic supply.

The quantity $I_R(t)$ was defined as the recharge current available to the battery. It is expressed

$$I_R(t) = H[I_{PV}(t) - I_L(t)](I_{PV}(t) - I_L(t)) \qquad [14]$$

It is proportional to the excess of the photovoltaic system supply beyond the load demand, when this quantity is positive, and zero when this quantity is negative.

We combine Eqs. (13) and (14) with Eqs. (1) through (7) describing the solar resource, Eq. (8) describing the photovoltaic power supply, and Eqs. (9) through (12) describing battery behavior to simulate the system. The following numerical example shows the results of some simulations.

## NUMERICAL EXAMPLE

To demonstrate the methodology described in the previous sections, a test case was simulated. This test case is based on an insolation model developed from data measured in Albuquerque, New Mexico (latitude ~35° North). It assumes the use of a non-concentrating, non-tracking array, tilted at an angle equal to the latitude. Each module of the array is rated at 2.3 amps (at standard test conditions), and three modules are connected in parallel for a total of 6.9 amps. The system includes a rechargeable battery rated at 12 volts and 105 amp-hours, and the load consists of one 18-watt lamp with an operational current of 1.9 amps. The load is applied for an average of 13 hours in the winter and 12 hours in the summer.

The analyses performed in this investigation were done within the Monte Carlo framework-that is, simulations of the random processes of interest were performed, and realizations were generated and stored. Statistical analyses were then performed on the realizations. The fundamental sub-process modeled as random in this study is the insolation random process. The randomness included in this sub-model causes most simulated quantities of interest in the overall model to also behave randomly.

The direct normal radiation and the diffuse horizontal radiation were modeled as components of a bivariate, first order Markov chain, as described above. We chose to model the system with 5x4=20 bivariate states; therefore, each joint realization of the direct normal radiation and the diffuse horizontal radiation could occupy any of 20 bins, and the two values would be represented as the values of the centroids of the bins. To check the accuracy of the model, we generated 100 one-year-long simulations and compared them to the raw, measured data. Figure 6a shows the measured total hourly insolation for January 1990, and Figure 6b shows a simulated total hourly insolation sequence of 31 January days. Their general character is similar; therefore, the simulation is plausible. (We should not expect the measurement and the simulation to be the same because they are simply two separate realizations from the same random source.)

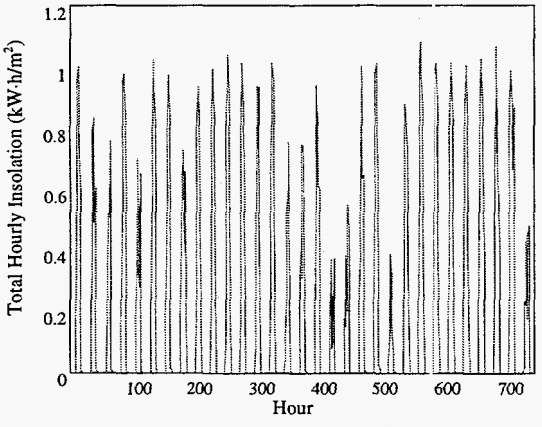


Figure 6a: Measured total hourly insolation for January 1990

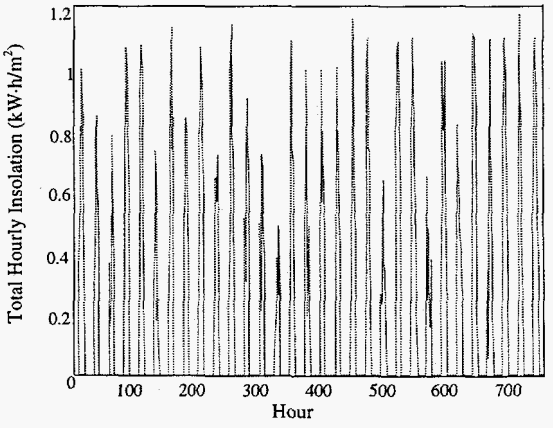


Figure 6b: Simulated total hourly insolation for 31 January days

There is a statistical means for comparing the simulations to the measurements, however. The measurements and the simulations were used to estimate the means, variances, and standard

deviations, as a function of time, on a January day and on a September day. The means minus one standard deviation, the means, and the means plus one standard deviation are shown in Figures 7a and 7b for the January day and the September day, respectively. The agreement appears satisfactory.

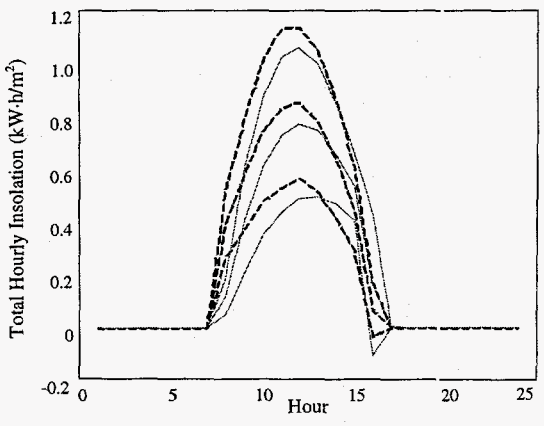


Figure 7a: Mean±1 standard deviation for January (solid-measured; dashed-simulated)

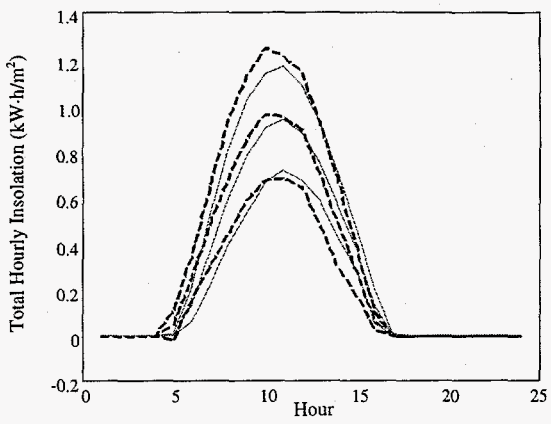


Figure 7b: Mean±1 standard deviation for Sept. (solid-measured; dashed-simulated)

The simulated insolation and the load profile serve as inputs for the rechargeable battery model. Through solution of the simultaneous governing equations, we generate 100 realizations of the charge/discharge cycle and also of the maximum potential capacity. Two sets of plots are shown in Figures 8a, 8b and 9a, and 9b of two of the time histories generated with this model.

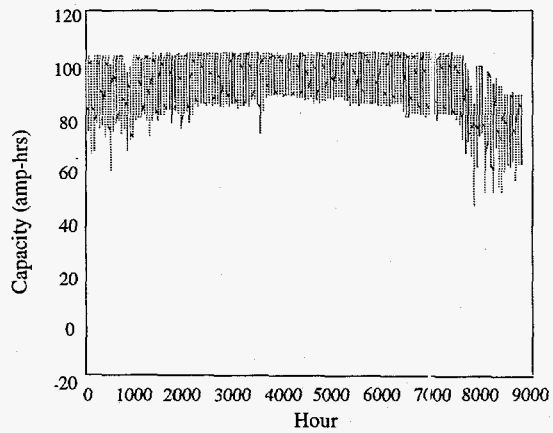


Figure 8a: Charge/discharge cycle for a battery that survived the entire year

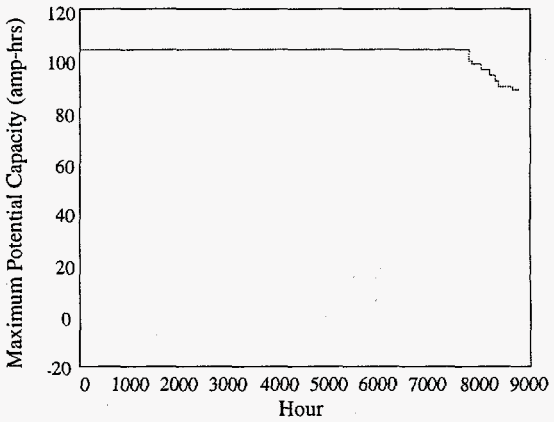


Figure 8b: Maximum potential capacity for the system in Figure 8a

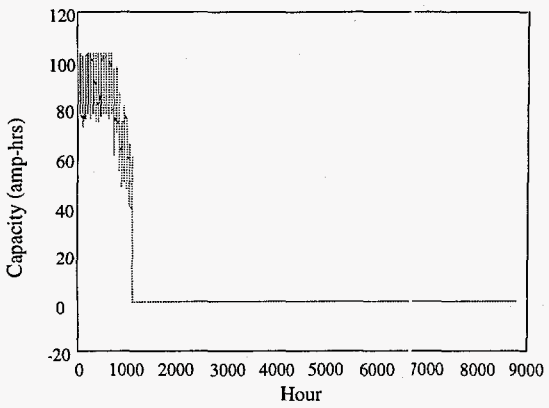


Figure 9a: Charge/discharge cycle for a battery that survived a fraction of the year

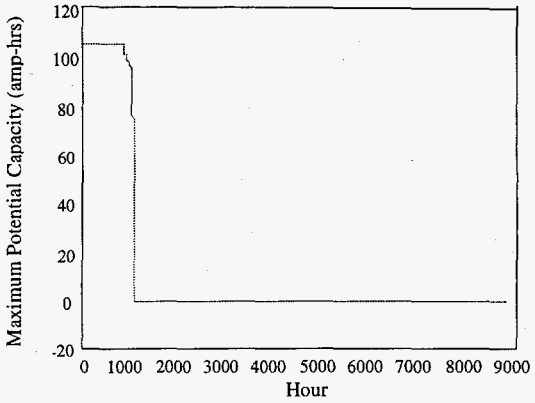


Figure 9b: Maximum potential battery capacity for the system in Figure 9a

From the resulting simulations the KDEs of the maximum potential capacity were obtained for two arbitrarily selected hours of the year (hours 1000 and 6000). These are shown in Figures 10a and 10b.

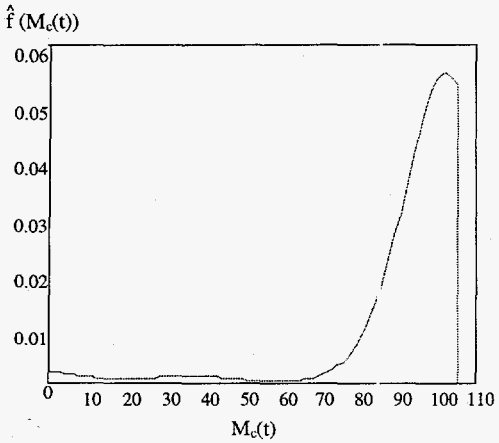


Figure 10a: KDE for the maximum potential capacity (@ hour 1000)

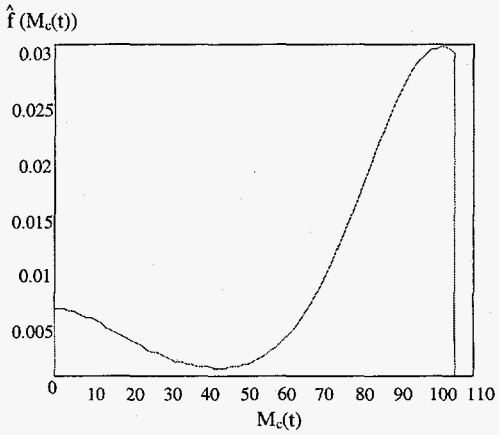


Figure 10b: KDE for the maximum potential capacity (@ hour 6000)

Figures 10a and 10b indicate a trend that shifts the probability mass of the maximum potential capacity toward zero. This occurs because as time progresses, some batteries fail. The fact that there is trough in the middle of the KDE in Figure 10b indicates that when a battery starts to fail, it progresses rapidly to total failure, $M_c(t) = 0$. This behavior is confirmed by Figure 9b. This shifting, and the rate at which it occurs, are characteristic of the power supply/storage/load system. Modification of system parameters would result in modification of the probabilistic character of the response measure.

## CONCLUSIONS

We have developed a framework for the probabilistic analysis of a power supply/storage/load system. In particular a solar resource and a rechargeable battery storage system have been modeled. The solar resource has been modeled as a bivariate random process using a Markov chain. Realizations were generated in the Monte Carlo framework. The rechargeable battery was modeled using a combination of classical equations and an artificial neural network. The simulations of battery behavior appear plausible but need to be validated.

Several steps need to be completed before the model can be implemented for practical system design. Most important, tests of rechargeable batteries need to be performed to calibrate the damage model embodied in the artificial neural network. Beyond this, the need for Monte Carlo simulation might be eliminated to yield a more efficient, direct analysis with the Markov chain model.

## ACKNOWLEDGMENT

Sandia National Laboratories is a multiprogram laboratory operated by Sandia Corporation, a Lockheed Martin Company, for the United States Department of Energy under Contract DE-AC04-94AL85000.

## REFERENCES

1. National Renewable Energy Laboratory, *National Solar Radiation Database User's Manual (1961-1990)*, version 1.1, (1994).
2. National Renewable Energy Laboratory's Analytic Studies Division, *Solar Radiation Data Manual for Flat-Plate and Concentrating Collectors*, (1994).
3. J. F. Kreider and F. Kreith, *Solar Energy Handbook*, pp. 2-1 - 2-18 and 2-72 - 2-73, McGraw Hill, New York, (1981).
4. R. Perez, P. Ineichen, R. Seals, J. Michalsky and R. Stewart, *Modeling Daylight Availability and Irradiance Components from Direct and Global Irradiance*, Solar Energy, Vol. 44, No. 5, pp. 271-289, (1990).
5. B. Silverman, *Density Estimation for Statistics and Data Analysis*, Chapman & Hall, Monographs on Statistics and Applied Probability 26, London, (1986).
6. Isaacson, D., Madsen, R., *Markov Chains: theory and Applications*, Wiley, New York, (1976).
7. C. C. O'Gorman, D. Ingersoll, R. G. Jungst and T. L. Paez, *Artificial Neural Network Simulation of Battery Performance*, Proceedings of the thirty-first Hawaii International Conference on System Sciences, IEEE, The University of Hawaii, Hawaii, Hawaii, (1998).
8. J. A. Freeman and D. M. Skapura, *Neural Networks, Algorithms, Applications, and Programming Techniques,* Addison-Wesley Publishing Company, Reading, Massachusetts, (1991).
9. J. Moody and C. Darken, "Fast Learning in Networks of Locally-Tuned Processing Units," *Neural Computation*, (1) 2, 281-294, (1989).